(6) Dee, G. T.; Walsh, D. J. *Macromolecules* **1988**, *21*, 815.
(7) Bank, M.; Leffingwell; Thies, C. J. *J. Polym. Sci.* **1972**, *A-2*, 1097.
(8) Nishi, T.; Wang, T. T.; Kwei, T. K. *Macromolecules* **1975**, *8*, 227.
(9) Snyder, H. L.; Meakin, P.; Reich, S. *Macromolecules* **1983**, *16*, 757.
(10) Halary, J. L.; Ubrich, J. M.; Nunzi, J. M.; Monnerie, L.; Stein, R. S. *Polymer* **1984**, *25*, 956.
(11) Lennard-Jones, J. E.; Devonshire, A. F. *Proc. R. Soc. (London)* **1937**, *A163*, 53.
(12) Prgogine, I. *The Molecular Theory of Solutions*; North Holland: Amsterdam, 1957.
(13) Ougizawa, T.; Walsh, D. J.; Dee, G. T., to be published.

Tracer Diffusion of Linear Polystyrenes in Dilute, Semidilute, and Concentrated Poly(vinyl methyl ether) Solutions

L. M. Wheeler† and T. P. Lodge*

Department of Chemistry, University of Minnesota, Minneapolis, Minnesota 55455.
Received October 12, 1988; Revised Manuscript Received February 1, 1989

ABSTRACT: Tracer diffusion coefficients, D, for four linear polystyrenes ($M_w = 6.5 \times 10^4$, 1.79×10^5, 4.22×10^5, and 1.05×10^6) have been measured in solutions of poly(vinyl methyl ether)/*o*-fluorotoluene, as functions of matrix molecular weight ($P_w = 1.4 \times 10^5$, 6.3×10^5, and 1.3×10^6) and matrix concentration ($0 \le c \le 0.30$ g/mL), by dynamic light scattering. The data have been corrected for the concentration dependence of the local friction, using pulsed-field-gradient NMR measurements of solvent diffusivity. The behavior of $D(M,P,c)$ is not consistent with the basic reptation-plus-scaling approach, in that a regime where $D \sim M^{-2}P^0c^{-1.75}$ is not observed. Apparent M exponents vary between −0.56 at very low c and −2.3 at relatively high P and c. A regime where D is independent of P is not established over this range of variables. The c dependence approaches power law behavior at high concentrations, where $D \sim c^{-3.3}$. All the data can be collapsed to a master curve when plotted as D/D_0 versus c/c', where c' is approximated as $(c^*_{PS}c^*_{PVME})^{0.5}$. The data can be interpreted in terms of a gradual transition to diffusion by reptation with increasing concentration, as suggested by more recent theoretical approaches. At the same time, however, it is not possible to eliminate other proposed mechanisms, such as those invoking cooperative chain motion or intermolecular hydrodynamic interactions, solely on the basis of measurements of D for linear polymers. In an accompanying article, measurements of D for 3-arm and 12-arm stars in the same matrix solutions are presented, which lend substantial support to the basic correctness of the reptation picture.

Introduction

The dynamics of polymers in semidilute and concentrated solutions remains a subject of considerable interest, as evidenced by both the number of experimental studies and the variety of theoretical approaches that have been brought to bear. The reptation postulate of de Gennes[1] has provided much of the impetus for recent work in this area, but it is certainly not yet established under what solution conditions reptation becomes the primary mode of polymer motion or even if it is necessary to invoke reptation in describing dynamics in solution. A good deal of attention has been directed toward experimental studies of the translational diffusion coefficient, D, because it is a property that may be defined for a single molecule and because the relevant models can make explicit predictions for the dependence of D on the diffusant molecular weight, M, the matrix molecular weight, P, and the matrix concentration, c.

There is no question that nondilute solutions are very difficult to treat theoretically. Unlike the limit of infinite dilution, where D is influenced primarily by intramolecular hydrodynamic interactions, or polymer melts, where D reflects mainly the mutual uncrossability of neighboring chains, D in solution involves both hydrodynamic and topological contributions. Furthermore, changes in local friction and in effective solvent quality with changing concentration can exert a significant influence on D. One consequence of this complexity is the necessity of making substantial assumptions in theoretical treatments. Another consequence is the danger inherent in extracting power law exponents from data; it is very difficult to vary M, P, or c by an order of magnitude without changing the solution conditions for which a given set of assumptions apply.

Theoretical approaches to the prediction of $D(M,P,c)$ may be classified into four categories. The first is the basic reptation-plus-scaling approach, in which the process of reptation, originally proposed for the motion of an unattached chain in a network, is assumed to apply in semidilute solutions; a straightforward scaling argument leads to the well-known predictions $D \sim M^{-2}c^{-1.75}$ and $D \sim M^{-2}c^{-3}$ for good-solvent and Θ-solvent conditions, respectively.[2] Implicit in this argument is the prediction that D is independent of P when $P \ge M$. The second category includes extensions and revisions of the basic reptation approach. Notable among these is the treatment of Hess,[3,4] who began with a Fokker–Planck equation describing the solution and arrived at the previous predictions as limiting behavior. The crucial assumption in this development is that hard-core repulsive interchain interactions constrain a given chain to move longitudinally. The even more recent model of Kavassalis and Noolandi[5-7] also recovers the reptation predictions in appropriate limits but makes the additional intriguing prediction that the concentration for the onset of entanglement, c_e, is always a factor of 8–10 larger than the overlap concentration, c^*. In contrast, the original scaling arguments do not consider c_e to be distinct from c^*. The third category includes models for which the dominant interaction is still topological, as is the case for reptation, but these interactions are reflected in the cooperative motions of neighboring chains. Somewhat rem-

* Author to whom correspondence should be addressed.
† Current address: Exxon Chemical Americas, Linden Technology Center, Linden, NJ 07036.

0024-9297/89/2222-3399$01.50/0

iniscent of the earlier ideas of Bueche,[8] the treatments of Fujita and Einaga[9] and of Kolinski et al.[10] fall into this category; so too does the application of the coupling model of Ngai et al.[11,12] to the dynamics of polymer liquids. Finally, the fourth category comprises the treatment of Phillies,[13-15] in which the importance of interchain hydrodynamic interactions is thought to outweigh that of the topological constraints significantly; the result is the stretched exponential dependence, $D/D_0 = \exp\{-\alpha c^u\}$, in which $0.5 \leq u \leq 1$ and α and u depend on M and P.

Experimental studies of $D(M,P,c)$ with which these models may be compared include those of Leger et al.,[16-18] Callaghan and Pinder,[19-21] Yu et al.,[22,23] von Meerwall et al.,[24] and Nose et al.,[25,26] as well as those from this laboratory;[27-29] the sedimentation and diffusion measurements of Nemoto et al. are also pertinent.[30,31] In their pioneering work, Leger, Hervet, and Rondelez used forced Rayleigh scattering (FRS) to measure the self-diffusion ($M = P$) of polystyrene (PS) in benzene and found reasonable agreement with $D \sim M^{-2}c^{-1.75}$.[16] However, in a later study, Marmonier and Leger determined that D exhibited a substantial P dependence until $P/M \geq 5$.[18] Only one of the other studies cited reported simultaneous observation of $M^{-2}c^{-1.75}$,[24] and the complete reptation-plus-scaling prediction ($D \sim M^{-2}P^0c^{-1.75}$) has never been seen. For example, Callaghan and Pinder reported $D \sim M^{-1.4}c^{-1.75}$ for PS ($M = P$) in CCl_4, using pulsed-field-gradient NMR.[21] Using FRS, Yu et al. found $D \sim M^{-2}$ for PS ($M = P$) in tetrahydrofuran, but no c scaling,[22] while for PS/toluene in the regime $P/M \geq 3$–5 the dependence on M approached $D \sim M^{-3}$.[23] As mentioned above, von Meerwall et al. also observed behavior consistent with $D \sim M^{-2}c^{-1.75}$ for $c > c_e$, after corrections for local friction were taken into account;[24] the system was PS/tetrahydrofuran and the measurements were made by NMR. Therefore, no measurements of the P dependence were possible. Nose et al. used dynamic light scattering from isorefractive solutions (DLS) to examine D for PS in poly(methyl methacrylate)/toluene solutions.[25,26] Because the two polymers are incompatible, only a limited concentration range could be examined, and very high molecular weights were employed to reach the entangled regime. Although the results were interpreted as being consistent with a crossover to reptation with increasing concentration, none of the three power laws ($D \sim M^{-2}P^0c^{-1.75}$) was explicitly demonstrated. In summary, all of these results are to a greater or a lesser degree consistent with a transition to a reptation regime as the solution concentration increases, but only under limited conditions are particular power laws observed. However, the increase in M and c dependence with increasing concentration can also be reconciled by most of the other categories of models identified above. Furthermore, the Phillies function has been shown to describe all of these data extremely well.[13-15] Thus, on the basis of all of these results, we do not believe it is possible to argue unequivocably either for or against the importance of reptation in semidilute or moderately concentrated solutions.

In our laboratory we have been using the ternary solution DLS technique to measure D for linear,[27-29] 3-arm star,[32] and 12-arm star[33] PS in poly(vinyl methyl ether) (PVME)/*o*-fluorotoluene (oFT) solutions. The solvent is chosen to be exactly isorefractive with PVME at 30 °C ($\partial n/\partial c \leq 0.001$) and is a good solvent for both polymers. Because PS and PVME are compatible, it has proven possible to make measurements up to at least $c = 0.30$ g/mL. The equivalence of D determined by FRS and by our method has recently been demonstrated.[34] In an earlier paper, we examined D for four linear PS ($M = 6.5 \times 10^4$, 1.79×10^5, 4.22×10^5, and 1.05×10^6) in a high-P PVME matrix (1.3×10^6) over the concentration range $0 \leq c \leq 0.10$ g/mL.[29] D was found to scale with $M^{-\beta}$ at all concentrations, with $\beta(c)$ changing smoothly from −0.56 at infinite dilution to −1.9 at the highest concentration examined; it was concluded that $c > c_e$ was definitely a necessary condition for dominant reptation-like behavior to be observed. Furthermore, it was demonstrated that a self-consistent combination of reptation and constraint release could not be invoked to describe the data. In this paper, we examine D for the same four PS in two additional PVMEs, with $P = 1.4 \times 10^5$ and 6.3×10^5, and extend the measurements for $P = 1.3 \times 10^6$ up to $c = 0.20$ g/mL. Measurements of the concentration dependence of the solution viscosity for $P = 1.3 \times 10^6$ are also reported. In addition, pulsed-field-gradient NMR has been used to determine the concentration dependence of the solvent diffusion, as an estimate of the changes in local friction. The results are discussed in terms of the models identified above.

The use of branched tracer polymers offers an additional, extremely powerful way to test these models, because only the reptation approach makes the explicit prediction that D(star) $\ll$ D(linear) in the reptation regime.[35] In a previous paper, we demonstrated that for 3-arm stars in the largest P matrix, the ratio D(star)/D(linear) decreased markedly with increasing c, providing strong evidence of the importance of diffusant architecture in determining D in entangled solutions.[32] This work has since been extended to the other PVMEs, as well as to 12-arm stars, and is discussed in the paper immediately following this one. In the second paper we also discuss static light scattering measurements of the concentration dependence of the coil dimensions for the PS tracers.

Experimental Section

Samples and Solutions. Four linear PS were used: NBS 1479, $M_w = 1.05 \times 10^6$; Toyo-Soda F-40, $M_w = 4.22 \times 10^5$; NBS 705, $M_w = 1.79 \times 10^5$; and Polysciences, $M_w = 6.5 \times 10^4$. The polydispersities were all less than 1.1. Three poly(vinyl methyl ether) (PVME) fractions were used in the dynamic light scattering (DLS) experiments, with $M_w = 1.3 \times 10^6$, 6.3×10^5, and 1.4×10^5 and polydispersities of approximately 1.6. The highest molecular weight PVME was also used for the NMR and viscosity measurements. The oFT solvent (Aldrich Chemical Co.) was filtered three times with 0.05-μm Millipore filters prior to use.

Details of the solution preparation protocol have been presented elsewhere.[29,33] Briefly, ternary solutions were prepared by combining dilute, filtered binary PS/oFT and PVME/oFT solutions. For the DLS measurements, the two solutions were mixed directly in a scattering cell and the solvent was evaporated off slowly, under flowing nitrogen, to achieve the desired initial PVME concentration. Since PVME is sensitive to oxidative degradation, a small amount (0.5% of the PVME concentration) of antioxidant, 4,4′-thiobis(6-*tert*-butyl-*m*-cresol) (Pfaltz & Bauer Co.), was added to each PVME stock solution. The subsequent ternary solutions were prepared by diluting with filtered PS stock solution, mixing thoroughly, and allowing sufficient time for equilibration. Selected measurements were repeated at 1-week intervals to ensure sample homogeneity. The PS concentrations were maintained at approximately $0.1c^*_{PS}$, where c^*_{PS}, the coil overlap concentration for the PS, was estimated from SLS data of PS in benzene.[36] At these small but finite probe concentrations, there is less than a 5% difference between the measured, mutual diffusion coefficient, D, and the tracer diffusion coefficient of the PS component, in this ternary system.[34] Therefore, there was no need to adjust the measured D values to $c_{PS} = 0$. Because of the dilution scheme, there was some fluctuation in c_{PS} for a given cell as a function of the PVME concentration, c. The mean and range of c_{PS} for each cell is listed in Table I. All DLS measurements were made at 30.0 ± 0.1 °C.

Table I
Mean and Range of PS Concentrations for Each Dilution Series

	c, mg/mL		
M	$P = 1.3 \times 10^6$	$P = 6.3 \times 10^5$	$P = 1.4 \times 10^5$
1.05×10^6	0.46 ± 0.01	0.47 ± 0.01	0.47 ± 0.02
4.22×10^5	0.76 ± 0.03	0.86 ± 0.02	0.82 ± 0.02
1.79×10^5	0.91 ± 0.01	1.77 ± 0.09	1.70 ● 0.09
6.5×10^4	3.08 ± 0.22	3.46 ± 0.25	3.54 ± 0.07

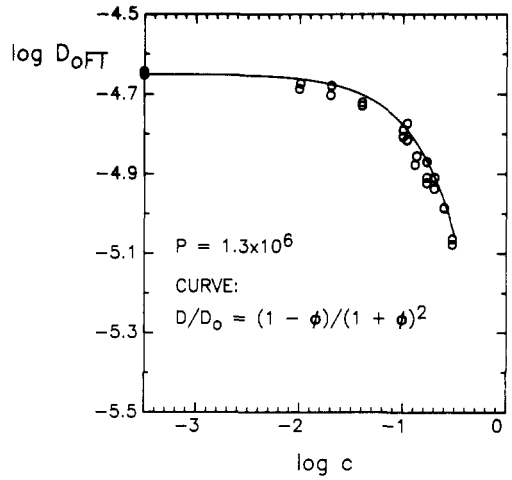

Figure 1. Solvent diffusivity as a function of PVME ($P = 1.3 \times 10^6$) concentration.

DLS Measurements. Data were collected on a home-built DLS spectrometer and a 136-channel multisample time correlator (Brookhaven Instruments BI-2030). Details of the apparatus and data analysis have been presented previously.[29,33,37] For each solution, correlation functions were accumulated in the homodyne mode at five or more scattering angles, and the decay rate was extracted with a second-order cumulant fit, using the experimental (measured) baseline. On the basis of previous extensive measurements on the same chemical system, with both cumulant analysis (using various base-line options) and the Provencher algorithm (CONTIN), supplemented with computer simulations of correlation functions, the decay rates extracted in this manner are estimated to be accurate to better than ±10%.[29] The diffusion coefficients were obtained from the slope of decay rate versus squared wave vector. Sample times were chosen to extend the data to 4–5 e-folds of the correlation function, but the early portion of the decay was emphasized. As has been discussed elsewhere, this approach minimizes the effects of probe polydispersity on the correlation function at higher matrix concentrations.[37]

NMR Measurements. Solvent diffusion in binary PVME/oFT solutions ($M_w = 1.3 \times 10^6$) was measured at 30 ± 0.3 °C by Fourier transform pulsed-field-gradient NMR. Samples were prepared in 4-mm NMR tubes by evaporating stock solutions to the desired concentrations in the range $0.02 \leq c \leq 0.3$ g/mL. Details of the experimental procedure and data analysis are given elsewhere.[38] The results are plotted in Figure 1 as log D_{oFT} versus log c over the range from 0.0 to 0.3 g/mL. By the highest concentration examined, D_{oFT} has fallen to 38% of its value in pure solvent, so the change in local friction, as estimated in this manner, is not great. Also included as a smooth curve in Figure 1 is the functional form $D/D_o = (1 - \phi)/(1 + \phi)^2$, where ϕ is the polymer volume fraction, which has been shown to describe the concentration dependence of solvent diffusion in a number of systems.[39]

Viscosity Measurements. The zero shear rate limiting viscosity, η, was measured for PVME/oFT solutions ($M_w = 1.3 \times 10^6$) over the concentration range from 0.0 to 0.2 g/mL. For $c \leq 0.04$ g/mL, the measurements were made at 30 ± 0.3 °C, using calibrated Schott-Gerate Ubbelohde viscometers and automatic timing mounts. Measurement times were all longer than 45 s and no kinetic energy corrections were applied. The viscosities of the higher concentration solutions were measured in a Rheometrics pressure rheometer at ambient temperature by extrapolating to zero shear rate data obtained between 0.001 and 10 s^{-1}. A pressure of 100 psi was maintained and solvent-saturated sponges were placed in the sample cup during the experiment to minimize solvent evaporation. Figure 2 shows a plot of log η versus log c over the measured concentration range and a fit to the stretched exponential form with η_s fixed as the measured solvent viscosity;

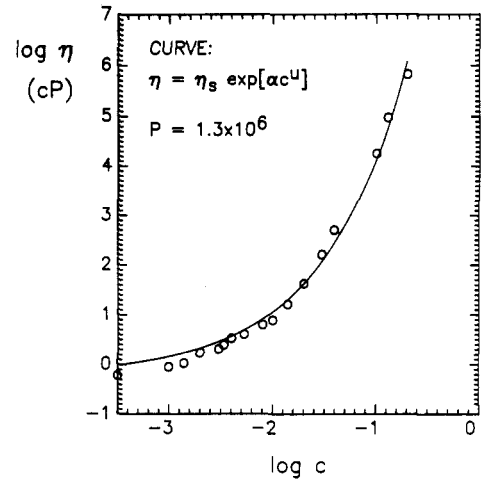

Figure 2. Solution viscosity as a function of concentration, for PVME ($P = 1.3 \times 10^6$) in oFT. The fitting function is indicated on the plot, with η_s fixed to the measured value of 0.612 cP.

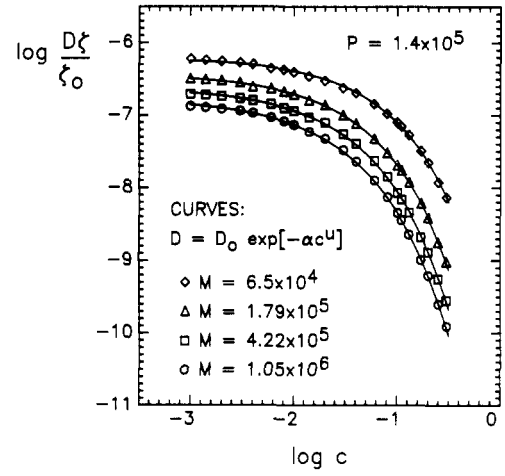

Figure 3. PS diffusivity, corrected for changing local friction, as a function of PVME concentration with $P = 1.4 \times 10^5$. The fitting function is indicated on the plot, with D_0 left as a floating parameter.

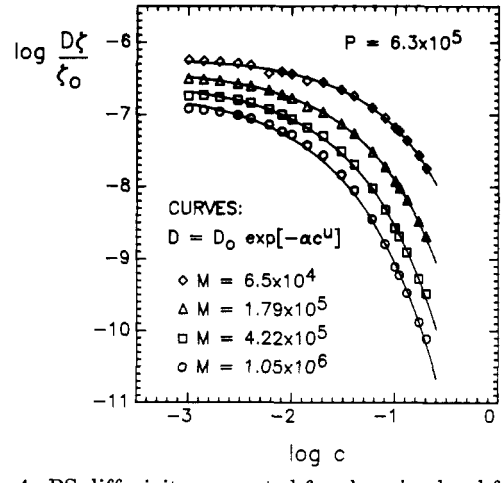

Figure 4. PS diffusivity, corrected for changing local friction, as a function of PVME concentration with $P = 6.3 \times 10^5$. The fitting function is indicated on the plot, with D_0 left as a floating parameter.

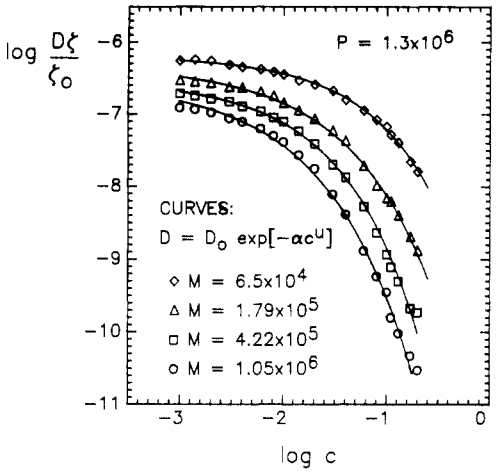

Figure 5. PS diffusivity, corrected for changing local friction, as a function of PVME concentration with $P = 1.3 \times 10^6$. The fitting function is indicated on the plot, with D_0 left as a floating parameter.

the fitting parameters are listed in Table V.

Results

In this section, the diffusion data will be presented and then examined in terms of the M, P, and c dependences. In the subsequent Discussion, the data will be examined in terms of the four categories of models identified in the Introduction.

In Figures 3, 4, and 5, log D is plotted as a function of log c for $P = 1.4 \times 10^5$, 6.3×10^5, and 1.3×10^6, respectively. In all cases, D has been scaled by the ratio $\zeta(c)/\zeta_0$, to account for the changing local friction. In this case, the local friction is estimated by $D_{oFT}(0)/D_{oFT}(c)$, following other workers.[24,40] Nevertheless, this approach should be viewed with some caution. Although the concentration dependence of the solvent diffusion clearly provides some measure of changes in local friction, it is not necessarily a unique measure or, therefore, the appropriate quantity to use. For example, it has been pointed out that solvent diffusion and viscoelastic experiments can yield different estimates of $\zeta(c)/\zeta_0$,[24] and recently it has been demonstrated that direct measurements of solvent relaxation and diffusion can give different values for this ratio.[41,42] However, as mentioned in the Experimental Section, the change in local friction as estimated in this way is rather small and thus should not exert a large influence on the data interpretation for this system.

Also included in Figures 3–5 are fits to the data using the stretched exponential form proposed by Phillies, with D_0 left as a floating parameter. The success and significance of these fits will be discussed subsequently; however, because this functional form appears to describe the data so well, it can be used as an interpolation formula. This is necessary in order to make comparisons among the data at fixed values of c, because the experimental protocol inevitably resulted in slightly different (less than 2%) exact values of c for different M and P combinations. The interpolated values of log D are also tabulated in Tables II, III, and IV, for $P = 1.4 \times 10^5$, 6.3×10^5, and 1.3×10^6, respectively. The data for $P = 1.3 \times 10^6$ and $c \leq 0.10$ g/mL are not tabulated, because they have been presented previously.[29]

***M* Dependence.** In Figures 6, 7, and 8 log D is plotted against log M at selected concentrations, in the $P = 1.4 \times 10^5$, 6.3×10^5, and 1.3×10^6 matrices, respectively. Because the interesting quantity is the M dependence at fixed c, no correction for changes in local friction should be necessary here. The data are represented by either filled or open symbols, depending on whether or not $c > c_e$ for both the PS tracer and the matrix. It can be seen that the M dependence for any given c and P combination is either close to a power law or concave up when plotted in the log–log format. For the two lower P matrices, lines with slopes of –0.56, –1, and–2 are drawn as a guide to the

Table II
Diffusion Coefficients for PS in PVME, $P = 1.4 \times 10^5$, Corrected for the Concentration Dependence of the Local Friction

	log $(D\zeta/\zeta_0)$, cm²/s			
log c, g/mL	$M = 1.05 \times 10^6$	$M = 4.22 \times 10^5$	$M = 1.79 \times 10^5$	$M = 6.5 \times 10^4$
D_0	−6.87	−6.68	−6.45	−6.22
−3.000	−6.88	−6.71	−6.49	−6.23
−2.854	−6.89	−6.72	−6.51	−6.24
−2.699	−6.91	−6.74	−6.52	−6.26
−2.523	−6.94	−6.77	−6.55	−6.28
−2.398	−6.97	−6.80	−6.61	−6.30
−2.222	−7.03	−6.85	−6.63	−6.36
−2.097	−7.08	−6.90	−6.67	−6.37
−2.000	−7.13	−6.94	−6.71	−6.41
−1.854	−7.23	−7.03	−6.79	−6.47
−1.699	−7.33	−7.11	−6.86	−6.53
−1.523	−7.48	−7.27	−7.00	−6.63
−1.398	−7.64	−7.39	−7.12	−6.69
−1.222	−7.90	−7.63	−7.32	−6.85
−1.097	−8.13	−7.85	−7.52	−6.98
−1.000	−8.35	−8.07	−7.69	−7.10
−0.959	−8.45	−8.17	−7.76	−7.16
−0.886	−8.65	−8.35	−7.93	−7.27
−0.770	−9.00	−8.69	−8.22	−7.50
−0.699	−9.21	−8.89	−8.42	−7.65
−0.602	−9.60	−9.26	−8.75	−7.93
−0.523	−9.91	−9.55	−9.02	−8.14

Table III
Diffusion Coefficients for PS in PVME, $P = 6.3 \times 10^5$, Corrected for the Concentration Dependence of the Local Friction

	log $(D\zeta/\zeta_0)$, cm²/s			
log c, g/mL	$M = 1.05 \times 10^6$	$M = 4.22 \times 10^5$	$M = 1.79 \times 10^5$	$M = 6.5 \times 10^4$
−3.000	−6.92	−6.74	−6.50	−6.25
−2.854	−6.94	−6.73	−6.52	−6.26
−2.699	−6.96	−6.76	−6.53	−6.27
−2.523	−7.01	−6.80	−6.57	−6.29
−2.398	−7.06	−6.84	−6.61	−6.32
−2.222	−7.14	−6.93	−6.67	−6.44
−2.097	−7.23	−7.00	−6.72	−6.41
−2.000	−7.28	−7.06	−6.77	−6.44
−1.854	−7.42	−7.18	−6.89	−6.53
−1.699	−7.56	−7.30	−6.97	−6.55
−1.522	−7.83	−7.51	−7.13	−6.66
−1.398	−8.05	−7.69	−7.26	−6.74
−1.222	−8.45	−8.02	−7.52	−6.91
−1.097	−8.79	−8.32	−7.73	−7.05
−1.000	−9.11	−8.57	−7.93	−7.18
−0.959	−9.23	−8.69	−8.02	−7.23
−0.886	−9.48	−8.91	−8.19	−7.36
−0.770	−9.89	−9.28	−8.48	−7.57
−0.699	−10.11	−9.48	−8.69	−7.74

Table IV
Diffusion Coefficients for PS in PVME, $P = 1.3 \times 10^6$, Corrected for the Concentration Dependence of the Local Friction

	log $(D\zeta/\zeta_0)$, cm²/s			
log c, g/mL	$M = 1.05 \times 10^6$	$M = 4.22 \times 10^5$	$M = 1.79 \times 10^5$	$M = 6.5 \times 10^4$
−0.959	−9.81	−9.11	−8.21	−7.29
−0.886	−10.02	−9.31	−8.40	−7.39
−0.770	−10.33	−9.68	−8.69	−7.66
−0.699	−10.53	−9.86	−8.88	−7.79

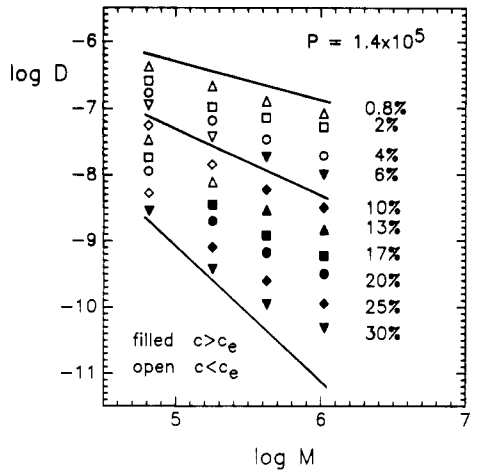

Figure 6. PS diffusivity as a function of PS molecular weight, at the PVME concentrations indicated on the plot, with $P = 1.4 \times 10^5$. The filled circles indicate data for which the matrix and the probe are entangled. The illustrative straight lines have slopes of −0.56, −1, and −2.

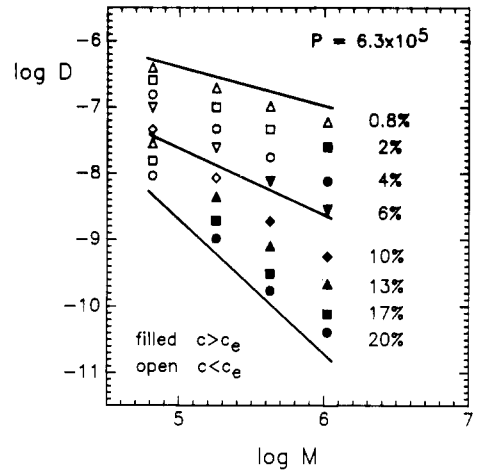

Figure 7. PS diffusivity as a function of PS molecular weight, at the PVME concentrations indicated on the plot, with $P = 6.3 \times 10^5$. The filled circles indicate data for which the matrix and the probe are entangled. The illustrative straight lines have slopes of −0.56, −1, and −2.

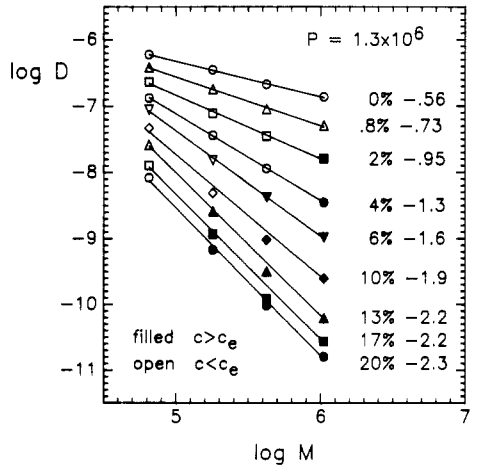

Figure 8. PS diffusivity as a function of PS molecular weight, at the PVME concentrations indicated on the plot, with $P = 1.3 \times 10^6$. The filled circles indicate data for which the matrix and the probe are entangled. The slopes of the straight lines, as obtained by linear regression, are indicated on the plot.

eye; in the largest P matrix, all the data have been force fit to a power-law dependence. The three slopes in Figures 6 and 7 are chosen to represent the infinite-dilution,

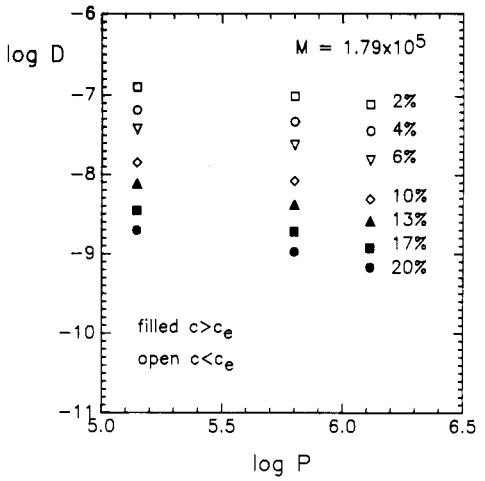

Figure 9. PS diffusivity, for $M = 1.79 \times 10^5$, as a function of PVME molecular weight, at the PVME concentrations indicated on the plot. The filled circles indicate data for which the matrix and the probe are entangled.

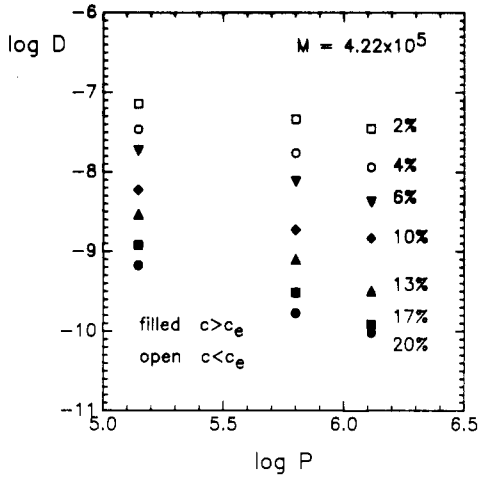

Figure 10. PS diffusivity, for $M = 4.22 \times 10^5$, as a function of PVME molecular weight, at the PVME concentrations indicated on the plot. The filled circles indicate data for which the matrix and the probe are entangled.

Rouse-like, and reptation conditions, respectively.

The general trends in the M dependence can be understood in the following way. At a given value of $c < c_e$ for the matrix, certainly no reptation should be observed at any value of M. Thus, for these data the slopes should lie between the −0.56 infinite-dilution limit when c is very small and the Rouse-like −1 when c is high enough to effectively screen the hydrodynamic interactions. This is consistent with the data. For the case where $c > c_e$ for both tracer and probe, then reptation becomes a possibility; this applies to the filled circles. Thus, in the limit of $M \ll P$, $D \sim M^{-2}$ should be observed if reptation applies, while for $M \gg P$, a return to a Stokes–Einstein regime is predicted.[43] In the latter event, an exponent between $M^{-0.5}$ and M^{-1} should obtain. This is indeed consistent with the data, as can be seen by considering the highest concentrations in each matrix. In Figure 6, the slope is greatest for small M, i.e., when $M \leq P$, and decreases as M increases. In Figure 7, the slope is closer to −2 over the entire range of M, as $M \leq P$ (at least in degree of polymerization, as discussed in the next section). In Figure 8, the force-fit slope at the highest concentration is −2.3, thus actually exceeding −2. This observation is not unprecedented, however; in both solution (with $P \gg M$)[23] and in the melt,[44,45] exponents of magnitude greater than 2 have been observed.

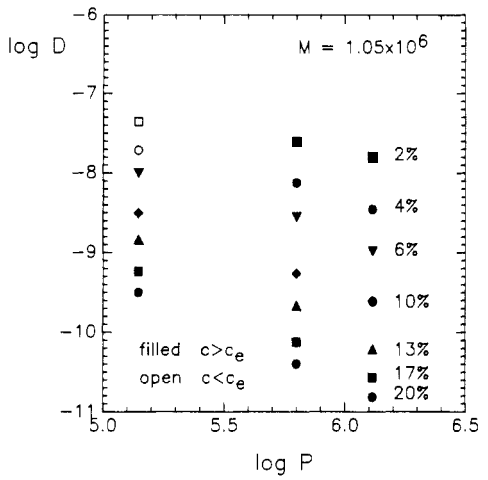

Figure 11. PS diffusivity, for $M = 1.05 \times 10^6$, as a function of PVME molecular weight, at the PVME concentrations indicated on the plot. The filled circles indicate data for which the matrix and the probe are entangled.

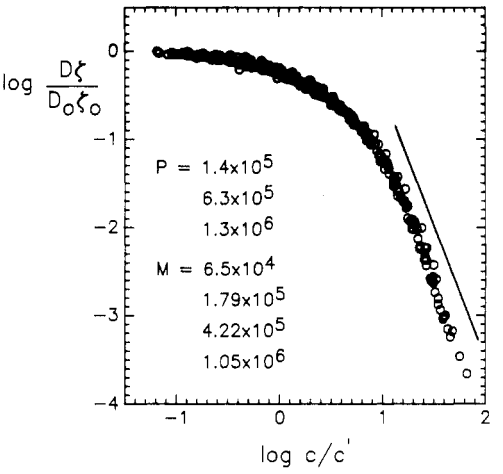

Figure 12. Normalized PS diffusivity, corrected for changing local friction, as a function of reduced PVME concentration. The interpretation of the reference concentration, c', is given in the text. The illustrative straight line has a slope of −3.

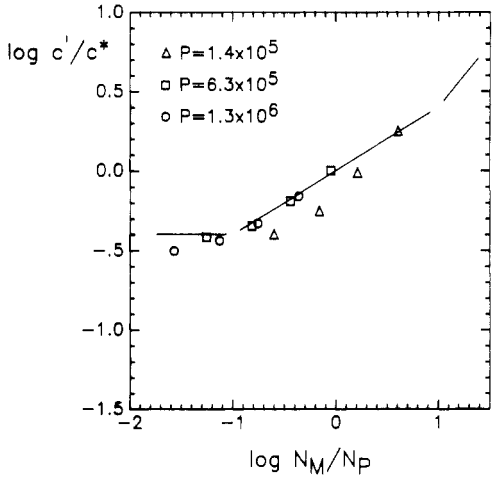

Figure 13. Reference concentration, c', normalized to c^* for each PS, as a function of the ratio of PS to PVME degree of polymerization. The illustrative straight lines have slopes of 0, 0.4, and 0.8, as discussed in the text.

***P* Dependence.** The dependence of D on P is illustrated in Figures 9, 10, and 11 for the 1.79×10^5, 4.22×10^5, and 1.05×10^6 PS, respectively. The log–log format is employed, and data are shown for selected concentrations across the measured range. The data for the smallest PS is not shown, because in this instance there is no appreciable P dependence at any concentration. From these data, it can be seen that there is a substantial P dependence at high concentrations, even though this is the regime where reptation is most likely to dominate. For example, at $c = 0.20$ g/mL a force fit to a power law dependence on P yields slopes of approximately −0.5, −1.0, and −1.4 for the three M values in increasing order. At lower concentrations, the dependence is always weaker. In the work of Kim et al.,[23] and also Leger and Marmonier,[18] P independence did not set in until $P/M \geq 3$–5. For the three PS examined here, this would correspond to P values of approximately 4×10^5, 8×10^5, and 2×10^6 for $M = 1.79 \times 10^5$, 4.22×10^5, and 1.05×10^6, respectively. These values were obtained from degree of polymerization rather than molecular weight, which is reasonable in this case because the ratio of entanglement molecular weights for PS to PVME is close to two,[45] as is the ratio of monomer molecular weights. Thus, only for the smallest of these three PS is the condition $P/M \geq 3$–5 satisfied for more than one value of P. Even in this case, however, a P-independent regime is not evident. One factor which may contribute to this is the polydispersity of the matrix. In other words, even when P_W/M_W is large enough, a substantial fraction of the matrix chains are considerably shorter than the average and thus more mobile. Nevertheless, it is clear that in these solutions, a regime where D scales approximately as M^{-2} is observed even though P independence is not established. At the same time, the P dependence is much weaker than the P^{-3} dependence claimed for constraint release in melts;[43] this is consistent with the argument presented previously.[29]

***c* Dependence.** Examination of the data in Figures 3–5 reveals that there are no obvious regions of power-law dependence on c, as may be expected for the reasons presented in the Introduction. However, it is possible to ask whether the data for different M and P can be scaled together in a revealing way. In Figure 12, all of the data in Figures 3–5 are plotted in the format $\log \{D(c)\zeta(c)/D_0\zeta_0\}$ versus $\log c/c'$, where D_0 is the infinite dilution value of D and c' is an arbitrary shift factor. In other words, c' is chosen to achieve the best superposition possible, using the data for $M = 1.05 \times 10^6$ and $P = 1.3 \times 10^6$ as a reference. The straight line on the plot has a slope of −3 and is a reasonable description of the c dependence over almost a decade in c; a force fit to the data gives a slightly steeper slope, approximately −3.3. If this straight line were extrapolated to its intersection with $(D\zeta/D_0\zeta_0) = 1$, a critical concentration of approximately $5c^*$ would be obtained.

Clearly, the reduction to a master curve in Figure 12 is excellent, which is a nontrivial result even if c' had no theoretical justification whatsoever. However, the values of c' employed can be rationalized in the following manner. If $M = P$, c' should be proportional to c^*. In the ternary system, both c^*_{PS} and c^*_{PVME} are relevant. For example, if $M \ll P$, the M chains could be much shorter than the matrix correlation length even though $c > c^*_{PVME}$ and thus move rather freely through the matrix. We can identify three limiting regimes: $M \gg P$, $M \approx P$, and $M \ll P$. In the former case, the time constant for M chain motion is much greater than for P chains, and thus the only tissue is whether the P chains are overlapped (or entangled). In other words, we would expect c' to scale with c^*_{PVME}. When $M \ll P$, the opposite situation prevails, and here the crucial question is whether the M chains are large enough to be overlapped (or entangled) with the P chains; thus, $c' \sim c^*_{PS}$. In the intermediate regime, the two overlap concentrations are similar and thus should be

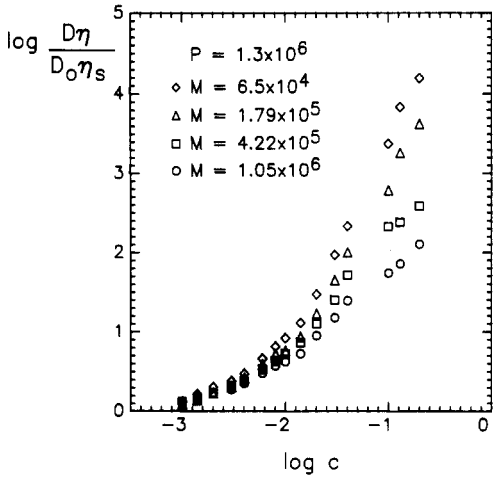

Figure 14. Normalized product of PS diffusivity and PVME solution viscosity, as a function of PVME concentration, for $P = 1.3 \times 10^6$.

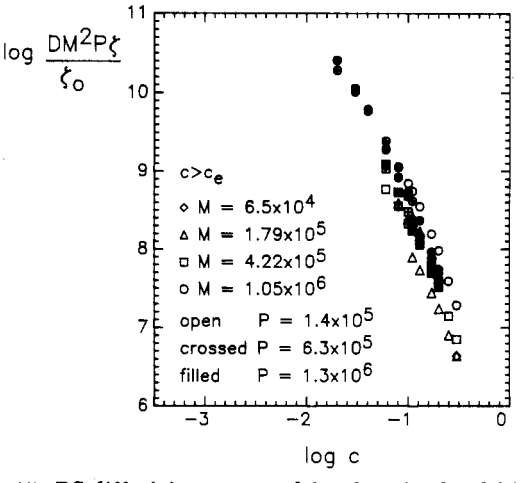

Figure 15. PS diffusivity, corrected for changing local friction and scaled by M^2P, as a function of PVME concentration, for the case where both the PS probe and the PVME matrix are entangled.

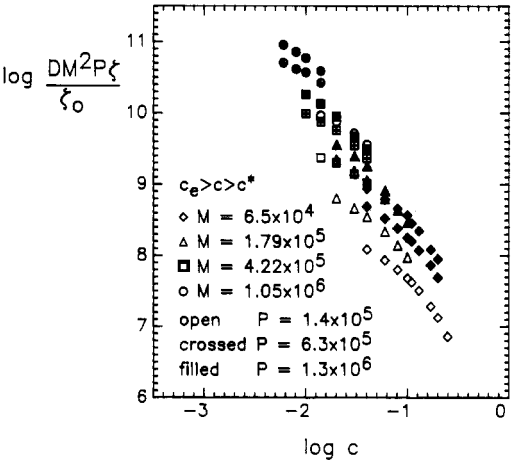

Figure 16. PS diffusivity, corrected for changing local friction and scaled by M^2P, as a function of PVME concentration, for the case where the matrix is semidilute but at least one of the two polymer components is not entangled.

significant. A "mixing rule" is required, and the form $(c^*_{PS}c^*_{PVME})^{0.5}$ is one reasonable possibility. In Figure 13, the values of c', normalized to c^*_{PS} such that $c' = c^*$ when $N_M = N_P$, are plotted logarithmically against log (N_M/N_P), where N is the degree of polymerization. The straight lines correspond to the scaling suggested above. Clearly, c' is at least approximately a universal function of M/P and is consistent with the argument presented. The range of M/P is not sufficiently great to determine the limiting behavior at either extreme.

One other way to examine the c dependence of D is to plot the product $D\eta$, normalized to the infinite dilution limit. This is illustrated in Figure 14, for $P = 1.3 \times 10^6$. The deviation from unity which is apparent at very low concentrations marks the end of the so-called "Stokes–Einstein" regime; it is apparent that the Stokes–Einstein regime is extremely limited. The reduction in D for the tracer PS chains is clearly less than the increase in η with increasing c, and the effect is more pronounced for lower M values. These results are entirely consistent with the results of other workers.

Discussion

In this section the results just presented are compared with the four categories of theoretical approach identified in the Introduction.

(i) Reptation plus Scaling. As pointed out in the Introduction, simultaneous observation of $M^{-2}P^0c^{-1.75}$ scaling has never been reported in the literature, and this statement is certainly not refuted by the data presented here. In general, the M dependence is not described by a simple power law over a wide range of M, but in the particular case of $P = 1.3 \times 10^6$, $P > M$ for all the samples examined, and power law behavior is observed. In this instance, the exponent varies smoothly down to a value of −2.3 (±0.2) at the highest concentration examined. Thus, this dependence appears to exceed the reptation prediction. As pointed out previously, such behavior has also been observed by Kim et al.[23] in the $P/M > 3$–5 regime and by Antonietti et al.[44] in melts. In the reptation picture, this may be rationalized as a crossover effect,[45] not unlike the $M^{3.4}$ scaling of the shear viscosity. In other words, in the molecular weight regime where reptation is beginning to become important, other processes enhance the mobility, so that D is larger than expected from a direct crossover to reptation. Then, as M increases and a reptation-dominated regime is finally achieved, the instantaneous M dependence must appear to be stronger than M^{-2}. The P dependence is also inconsistent with a picture of dominant reptation, but at the same time it must be borne in mind that the $P \gg M$ limit is not reached for these samples. Finally, the c dependence is close to −3 over a significant range of concentration, as indicated in Figure 12. The predicted $c^{-1.75}$ scaling in the semidilute regime is definitely not observed.

(ii) Modified Reptation Models. The model of Hess[3,4] has some features that are consistent with these results. In general, this model predicts a much more gradual crossover to reptation with increasing concentration. Also, the constraint release dependence on P should be closer to P^{-1}, rather than the P^{-3} envisioned in the melt. Thus, to test this hypothesis the data can be plotted as log $DM^2P\zeta/\zeta_0$ versus log c, as shown in Figures 15 and 16. In Figure 15, the data are distinguished by the fact that the concentration is high enough so that the probe and matrix are both above their respective c_e's, while in Figure 16 they fall in an intermediate semidilute but not entangled regime, i.e., $c^* \leq c \leq c_e$. In other words, the matrix concentration is semidilute, but either the probe or the matrix (or both) are not entangled. The entanglement concentration, c_e, is estimated as $\rho M_e^0/M$, where ρ is the polymer density and M_e^0 is the molecular weight between entanglements for the bulk polymer (7200 for PVME and 18000 for PS). It can be seen that the entangled solution data do reduce to a master curve, albeit not a very good one,

while the not entangled but still semidilute data clearly do not.

From the above discussion it can be seen that the results are generally consistent with the reptation picture, as further developed by Hess.[3,4] However, the results presented here should certainly not be viewed as compelling evidence in favor of this model. For instance, the Hess model has two limits with varying M and P: $D \sim M^{-2}P^0$ in the dominant reptation regime and $D \sim M^{-1}P^{-1}$ in the dominant constraint release regime. Thus, an apparent scaling of $D \sim M^{-2}P^{-1}$ as suggested by Figure 15 is not identical with either limit. In addition, Nemoto et al. have recently shown that their sedimentation data could be reduced to a master curve, following the detailed Hess model predictions, by assuming that the hydrodynamic and topological contributions to diffusion could be separated.[30,31] A universal "topological function" was obtained by assuming that a chain of one-tenth the concentration-dependent entanglement molecular weight exhibited Rouse-like diffusion ($D \sim M^{-1}$) only and by using the mobility of those chains to normalize the diffusion coefficients obtained for longer chains. This analysis is not at all successful in reducing our data to a master curve, however; the reason for this difference is not yet clear.

One clear conclusion which may be drawn from the results in Figures 15 and 16 is that the concept of a semidilute but not entangled regime is valid. In other words, the concentration for the onset of semidilute behavior in static properties, such as the osmotic pressure, is appreciably less than the concentration at which the dynamics reveal the effects of topological constraints. This is in good agreement with the results of von Meerwall et al.[24] and Callaghan and Pinder,[21] as well as the picture of Ferry.[46] However, Leger and Marmonier found no evidence for such a regime.[18] It is interesting to note that the recent model of Kavassalis and Noolandi not only predicts the existence of this regime, but also estimates it to extend over as much as a decade in concentration;[5-7] this is perhaps slightly greater than the range implied by our results.

(iii) Cooperative Chain Motion Models. This section will be necessarily brief, as the models in this category have not been extended to the point of providing specific predictions for tracer diffusion in ternary polymer solutions. Nevertheless, in the melt they are able to rationalize to some extent the observed M dependences for D and η, and it is reasonable to expect that they could be successfully extended to the solution case. However, these approaches currently suffer from a major limitation, namely, that in the melt they provide no mechanism by which the reduced mobility of star-branched polymers is explained. As will be discussed at length in the following paper, this reduction in D for star polymers is also observed in entangled solutions; this must be taken as strong support for mechanisms of motion that are sensitive to diffusant architecture. To date, only the reptation and the coupling models satisfy this criterion, as far as we are aware.

In addition to the models of Fujita and Einaga[9] and Kolinski et al.,[10] the coupling model approach of Ngai et al.[11,12] was assigned to this category. This is perhaps a little misleading, because this model makes no attempt to describe a detailed mechanism for polymer motion in entangled systems. Rather, it is a very general way of understanding the dynamics of cooperative systems and has been applied to a number of polymer problems. The diffusion of polymers, both linear and branched, in solution and in the melt has recently been examined extensively in this context;[47] thus no further discussion will be presented here. However, the coupling model is able to rationalize the different temperature dependences of D for star and linear polymers,[47] an experimental observation that is not addressed by most models of polymer dynamics.

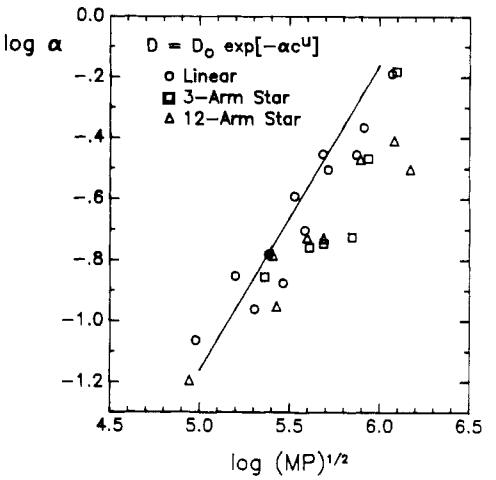

Figure 17. Values of α from the function indicated on the plot, for linear, 3-arm star, and 12-arm star PS diffusivity, as a function of $(MP)^{0.5}$. The illustrative straight line has a slope of 1.

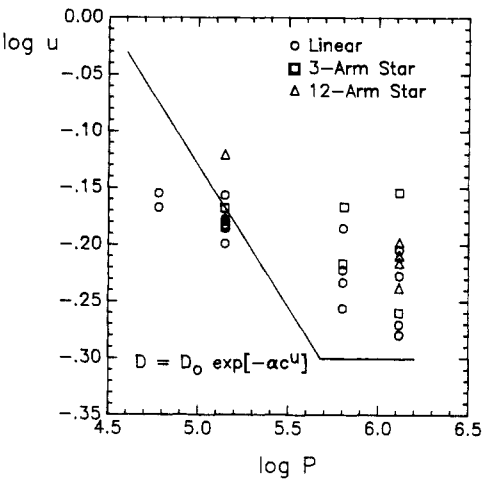

Figure 18. Values of u from the function indicated on the plot, for linear, 3-arm star, and 12-arm star PS diffusivity, as a function of P. The illustrative straight line is described in the text.

(iv) Phillies Model. This approach stands in stark contrast to all the preceding treatments, because it emphasizes intermolecular hydrodynamic interactions over topological constraints;[13-15] one consequence of this is that it has not been able to justify the presence of a plateau in the elastic shear modulus for entangled solutions and melts. For this reason, among others, the model has not met with universal acceptance, even though it is extremely successful in describing the concentration dependence of D. It is certainly the case that all of the data presented here, and in the following paper, are well-described by the stretched exponential form. In a previous paper it was concluded that this probably reflected more the flexibility of the stretched exponential as a fitting function than the correctness of the underlying physics.[29] However, it is interesting to note that the stretched exponential concentration dependence does appear as a natural consequence of the coupling model description of diffusion.[47]

Since the original observation that this functional form described a large body of data, some additional analysis has led to predictions for the dependence of the parameters α and u on M and P. Specifically, α is predicted to scale with $(MP)^{0.5}$ and u should exhibit a crossover from 0.5 at large P to 1.0 at small P, independent of M.[14] In Figures

Table V
Phillies Parameters for Linear PS Using Floated and Fixed D_0[a]

P	M	$10^7 D_0$	α, g/mL	α, mg/mL	u
		Floated D_0			
1.3×10^6	1.05×10^6	2.76	22.9	0.645	0.525
	4.22×10^5	2.89	20.8	0.350	0.592
	1.79×10^5	4.63	14.2	0.351	0.536
	6.5×10^4	6.25	9.89	0.133	0.624
6.3×10^5	1.05×10^6	2.16	19.8	0.430	0.554
	4.22×10^5	2.81	17.7	0.312	0.584
	1.79×10^5	4.08	14.0	0.255	0.599
	6.5×10^4	5.90	9.88	0.109	0.652
1.4×10^5	1.05×10^6	1.70	15.6	0.198	0.632
	4.22×10^5	2.40	14.9	0.165	0.652
	1.79×10^5	3.64	13.3	0.140	0.663
	6.5×10^4	6.08	10.2	0.086	0.697
		Fixed D_0			
1.3×10^6	1.05×10^6	1.36	26.9	0.321	0.641
	4.22×10^5	2.11	19.6	0.439	0.650
	1.79×10^5	3.51	15.5	0.234	0.607
	6.5×10^4	5.98	10.2	0.118	0.646
6.3×10^5	1.05×10^6	1.36	21.7	0.266	0.637
	4.22×10^5	2.11	19.1	0.217	0.648
	1.79×10^5	3.51	14.5	0.178	0.637
	6.5×10^4	5.98	9.81	0.113	0.646
1.4×10^5	1.05×10^6	1.36	16.0	0.150	0.676
	4.22×10^5	2.11	15.3	0.139	0.681
	1.79×10^5	3.51	13.4	0.129	0.672
	6.5×10^4	5.98	10.3	0.080	0.704

P		η_s, cP	α, g/mL	α, mg/mL	u
1.3×10^6	floated	0.160	32.5	1.50	0.445
	fixed	0.612	34.4	0.852	0.536

[a] Fit to data corrected for $\zeta(c)$.

17 and 18, we have plotted all the values of α and u, respectively, that we have obtained for linear PS, 3-arm stars, and 12-arm stars diffusing in four PVME matrices (the fourth $P = 6 \times 10^4$), along with the predicted dependences. The values of α and u for the linear PS are also listed in Table V, as obtained by nonlinear regression, with D_0 both fixed to the measured value and also allowed to float. For α, the dependence on $(MP)^{0.5}$ is not consistent with the data, at least in the sense that if the data were fit to a power-law dependence on the product (MP), a slope much less than 0.5 would be obtained. However, this view is a little bit misleading, because the scale of the plot is quite expanded. In other references, the values of α range over at least three decades of the ordinate and taken as a whole are quite close to the predicted power law. There is a more substantial disagreement in Figure 18, however. Here it can be seen that u almost always lies between 0.6 and 0.7, and there is not much suggestion of a P dependence. This observation is in fact inherent in Figure 12, as there would be no way to scale all the data together merely by a shift along the concentration axis if the values of u differed by very much. In ref 14, a plot of u versus P is taken as evidence for the correctness of the predicted crossover. However, the format of that plot is such as to completely mask the fact that the u values are widely scattered and even approach values as high as 1.5. The stretched exponential function is rather sensitive to changes in either α or u, and the uncertainty in the experimental data is generally much too small to generate noticeable error bars on the values of α and u extracted. Thus, the wide scatter seen in the values of α and u, relative to the curves in Figures 17 and 18, must result from inadequacies in the theory and not experimental error. In Table V, it is also apparent that D_0 values obtained from fitting to the stretched exponential are systematically greater than the measured values, by as much as a factor of 2. This was observed previously[29] and attributed to a postulated PS coil contraction with increasing matrix concentration. However, although such a coil contraction has now been confirmed experimentally, and discussed in the following paper, it cannot be invoked to explain the differences between D_0(float) and D_0(measured). The reason is that the derivation of the stretched exponential advanced by Phillies[14] already incorporates the probe coil contraction, and thus it should not be incorporated twice. This may be viewed as additional evidence that this derivation is not entirely adequate.

Summary

The tracer diffusion coefficients, D, for four linear polystyrene (PS) molecular weights, M, have been examined in solutions of three different molecular weight poly(vinyl methyl ether) (PVME) matrices, P, under dilute, semidilute, and concentrated conditions. In addition, measurements of solution viscosity and solvent diffusion have been undertaken. The results have been discussed in terms of the M, P, and c dependences of D and then compared with four categories of theoretical treatment. Some of the salient conclusions are the following:

1. The M dependence of D is not a simple power law in general, but in the highest P solutions apparent power-law behavior is seen. In this case, the exponent decreases very smoothly from −0.56 in dilute solution to approximately −2.3 at the highest concentration examined. The regime where D scales approximately with M^{-2} does not begin until concentrations well beyond the onset of semidilute behavior in static properties.

2. The values of D are not independent of P over the range examined, in contrast to the simple reptation picture. Generally, D decreases weakly with increasing P, even at the highest concentrations, and with a much weaker dependence than predicted by the constraint release model as applied to melts. The regime $P/M > 3$–5, where D has been found to be independent of P, was not investigated thoroughly, due to limits on the available PVME molecular weights. Also, the polydispersity of the matrix probably contributes to the P dependence.

3. The concentration dependence was universal, in the sense that all the data scaled to a master curve by using an arbitrary reference concentration, c'. It was also shown that c' was well-approximated as $(c^*_{PS}c^*_{PVME})^{0.5}$ over most of the measured range. No evidence of $c^{-1.75}$ scaling was observed, but in the higher concentrations D scaled with approximately $c^{-3.3}$ over an appreciable range of concentration.

4. The basic reptation-plus-scaling picture for D in semidilute solutions is not supported by these data; a regime where $D \sim M^{-2}P^0c^{-1.75}$ is not observed. However, the "modified reptation" arguments of Hess[3,4] and Kavassalis and Noolandi[5-7] make predictions that are more consistent with the results. For example, the Hess treatment predicts a rather broad transition to a reptation regime with increasing concentration, with a dependence of P^{-1}, which is closer to what is observed experimentally. The existence of a semidilute but not entangled regime, as predicted for example by Kavassalis and Noolandi, is also indicated by these data.

We believe that it is not possible to eliminate any of the four categories of models from consideration solely on the basis of the data presented here and on the basis of other measurements of D in similar concentration regimes, even though they rest on fundamentally different assumptions. However, this apparently rather disappointing conclusion is modified when other experiments are taken into consideration. Most importantly, of these four theoretical

approaches, only the reptation-based pictures make the specific prediction that branched molecules should diffuse considerably less rapidly than linear polymers, under comparable conditions. This prediction has received considerable support from measurements of melt diffusion of stars, and in the following paper, we discuss the diffusion of 3-arm and 12-arm stars in entangled solutions. When compared with the data in this paper, it becomes clear that, at the very least, an architecture-dependent diffusion mechanism is operative in entangled polymer solutions. Thus, the models that are consistent with the limiting reptation behavior, but that also make more realistic predictions for the M, P, and c dependences, should definitely be considered as the most promising. It is particularly unfortunate, perhaps, that the model of Hess,[3,4] while seemingly in good agreement with the diffusion behavior of linear polymers, cannot be extended directly to the case of branched polymers.

Acknowledgment. Acknowledgment is made to the donors of The Petroleum Research Fund, administered by the American Chemical Society, for support of this research. L.M.W. is grateful to the Graduate School of the University of Minnesota for fellowship support. The assistance of W. G. Miller, H. Dai, J.-F. Bodet, and R. Olayo with the NMR measurements and S. Olson with the viscosity measurements is appreciated.

Registry No. PS, 9003-53-6; PVME, 9003-09-2.

References and Notes

(1) de Gennes, P.-G. *J. Chem. Phys.* **1971**, *55*, 572.
(2) de Gennes, P.-G. *Scaling Concepts in Polymer Physics*; Cornell University: Ithaca, NY, 1979.
(3) Hess, W. *Macromolecules* **1986**, *19*, 1395.
(4) Hess, W. *Macromolecules* **1987**, *20*, 2587.
(5) Kavassalis, T. A.; Noolandi, J. *Phys. Rev. Lett.* **1987**, *59*, 2674.
(6) Kavassalis, T. A.; Noolandi, J. *Macromolecules* **1988**, *21*, 2869.
(7) Kavassalis, T. A.; Noolandi, J., submitted for publication in *Macromolecules*.
(8) Bueche, F. *J. Chem. Phys.* **1952**, *20*, 1959.
(9) Fujita, H.; Einaga, Y. *Polym. J. (Tokyo)* **1985**, *17*, 1131.
(10) Kolinski, A.; Skolnick, J.; Yaris, R. *J. Chem. Phys.* **1988**, *88*, 1407.
(11) Ngai, K. L.; Rendell, R. W.; Rajagopal, A. K.; Teitler, S. Conference on Dynamic Aspects of Structural Change in Liquids and Glasses. *Ann. N.Y. Acad. Sci.* **1985**, *484*, 150.
(12) Rendell, R. W.; Ngai, K. L.; McKenna, G. B. *Macromolecules* **1987**, *20*, 2250.
(13) Phillies, G. D. J. *Macromolecules* **1986**, *19*, 2367.
(14) Phillies, G. D. J. *Macromolecules* **1987**, *20*, 558.
(15) Phillies, G. D. J.; Peczak, P. *Macromolecules* **1988**, *21*, 214.
(16) Leger, L.; Hervet, H.; Rondelez, F. *Macromolecules* **1981**, *14*, 1732.
(17) Deschamps, H.; Leger, L. *Macromolecules* **1986**, *19*, 2760.
(18) Marmonier, M. F.; Leger, L. *Phys. Rev. Lett.* **1985**, *55*, 1078.
(19) Callaghan, P. T.; Pinder, D. N. *Macromolecules* **1980**, *13*, 1085.
(20) Callaghan, P. T.; Pinder, D. N. *Macromolecules* **1981**, *14*, 1334.
(21) Callaghan, P. T.; Pinder, D. N. *Macromolecules* **1984**, *17*, 431.
(22) Wesson, J. A.; Noh, I.; Kitano, T.; Yu, H. *Macromolecules* **1984**, *17*, 431.
(23) Kim, H.; Chang, T.; Yohanan, J. M.; Wang, L.; Yu, H. *Macromolecules* **1986**, *19*, 2737.
(24) von Meerwall, E. D.; Amis, E. J.; Ferry, J. D. *Macromolecules* **1985**, *18*, 260.
(25) Numasawa, N.; Hamada, T.; Nose, T. *J. Polym. Sci., Part B: Polym. Phys.* **1986**, *24*, 19.
(26) Numasawa, N.; Kuwamoto, K.; Nose, T. *Macromolecules* **1986**, *19*, 2593.
(27) Lodge, T. P. *Macromolecules* **1983**, *16*, 1393.
(28) Hanley, B.; Tirrell, M.; Lodge, T. P. *Polym. Bull. (Berlin)* **1985**, *14*, 137.
(29) Wheeler, L. M.; Lodge, T. P.; Hanley, B.; Tirrell, M. *Macromolecules* **1987**, *20*, 1120.
(30) Nemoto, N.; Okada, S.; Inoue, T.; Kurata, M. *Macromolecules* **1988**, *21*, 1502.
(31) Nemoto, N.; Okada, S.; Inoue, T.; Kurata, M. *Macromolecules* **1988**, *21*, 1509.
(32) Lodge, T. P.; Wheeler, L. M. *Macromolecules* **1986**, *19*, 2983.
(33) Lodge, T. P.; Markland, P. *Polymer* **1987**, *28*, 1377.
(34) Chang, T.-Y.; Han, C. C.; Wheeler, L. M.; Lodge, T. P. *Macromolecules* **1988**, *21*, 1870.
(35) de Gennes, P.-G. *J. Phys. (Les Ulis, Fr.)* **1975**, *36*, 1199.
(36) Miyaki, Y.; Einaga, Y.; Fujita, H. *Macromolecules* **1978**, *11*, 1180.
(37) Lodge, T. P.; Wheeler, L. M.; Hanley, B.; Tirrell, M. *Polym. Bull. (Berlin)* **1986**, *15*, 35.
(38) Bodet, J.-F.; Bellare, J. R.; Davis, H. T.; Scriven, L. E.; Miller, W. G. *J. Phys. Chem.* **1988**, *92*, 1898.
(39) Blum, F. D.; Pickup, S.; Foster, K. R. *J. Colloid Interface Sci.* **1986**, *113*, 336.
(40) Nemoto, N.; Landry, M. R.; Noh, I.; Kitano, T.; Wesson, J.; Yu, H. *Macromolecules* **1985**, *18*, 308.
(41) von Meerwall, E. D.; Amelar, S.; Smeltzly, M. A.; Lodge, T. P. *Macromolecules* **1989**, *22*, 295.
(42) Morris, R. L.; Amelar, S.; Lodge, T. P. *J. Chem. Phys.* **1988**, *89*, 6523.
(43) Daoud, M.; de Gennes, P.-G. *J. Polym. Sci., Polym. Phys. Ed.* **1979**, *17*, 1971.
(44) Antonietti, M.; Coutandin, J.; Sillescu, H. *Macromolecules* **1986**, *19*, 793.
(45) Watanabe, H.; Kotaka, T. *Macromolecules* **1987**, *20*, 530.
(46) Ferry, J. D. *Viscoelastic Properties of Polymers*, 3rd ed.; *Wiley*: New York, 1980.
(47) Ngai, K. L.; Lodge, T. P., submitted for publication in *J. Chem. Phys.*